



Formation of solid and hollow cuprous oxide nanocubes in water-in-oil microemulsions controlled by the yield of hydrated electrons

Qingde Chen, Xinghai Shen*, Hongcheng Gao

Beijing National Laboratory for Molecular Sciences, Department of Applied Chemistry, College of Chemistry and Molecular Engineering, Peking University, Beijing 100871, People's Republic of China

Received 14 December 2006; accepted 17 March 2007

Available online 3 May 2007

Abstract

A local ordered structure constructed from solid Cu_2O nanocubes was obtained by the radiolytic reduction of $\text{Cu}(\text{NO}_3)_2$ in a water-in-oil (W/O) microemulsion composed of Triton X-100, *n*-hexanol, cyclohexane, and water in the presence of ethylene glycol (EG). However, when Triton X-100 was replaced with Brij 56 in the microemulsion, hollow Cu_2O nanocubes were synthesized. The addition of toluene into the Brij 56 system could decrease the ratio of hollow nanocubes. It was suggested that the balance between the reduction rate of Cu^{2+} depending on the yield of hydrated electrons (e_{aq}^-) and the escape rate of the mixed solvent determined their final morphologies. The presence of EG influenced the rigidity of the interface of the microemulsion and thus the above balance, which resulted in the different morphologies of Cu_2O nanoparticles in the Brij 56-based microemulsion.

© 2007 Elsevier Inc. All rights reserved.

Keywords: Cuprous oxide; Nanocubes; γ -Irradiation; Hydrated electrons; Microemulsion

1. Introduction

In the field of nanoscience and nanotechnology, the largest activity has been focused on the synthesis of new nanoparticles with different sizes and new shapes, which have strong effects on their widely varying properties [1,2]. Among the numerous materials, hollow materials with nanometer-to-micrometer dimensions have attracted much attention for their tailored structural, optical, mechanical, and surface properties and therefore their wide range of potential applications, such as controlled delivery, photonic crystals, fillers, and catalysts [3–8]. So far, many methods have been explored to synthesize hollow materials: “hard templates” (polystyrene spheres [3–5], silica spheres [6], metal nanoparticles [7,9], carbon nanotubes [10], etc.), “soft templates” (normal micelles [8,11,12], block copolymer micelles [13,14], polymer [15,16], microemulsions [17], etc.), in situ templates [18], and template-free methods [19–21]. However, most efforts have been made

to synthesize hollow spheres [3–7,9,13,15,16,18,20] and nanotubes [7,10,14,16,20]. There are only a few reports on hollow nanocubes [7,8,11,21,22].

γ -Irradiation has been widely used in preparing nanoparticles [23,24]. Now, there are several reports about the synthesis of hollow structures via this method [17,25,26]. However, they are limited to hollow spheres. In our previous work, we reported that the radiolytic reduction of Cu^{2+} in W/O microemulsions was well controlled by adjusting the yield of hydrated electrons (e_{aq}^-) [27]. Meanwhile, we found that it should be possible to control the shape of nanoparticles in the same way [27]. To get deep insight into this issue, it is necessary to choose two similar systems in which the yield of e_{aq}^- is obviously different, whereas other effects are identical to a great extent. For this purpose, Triton X-100 and Brij 56, whose structures are similar, were selected to construct W/O microemulsions with *n*-hexanol, cyclohexane, and water in the presence of ethylene glycol (EG). In the present paper, the radiolytic syntheses of

* Corresponding author. Fax: +86 10 62759191.
E-mail address: xshen@pku.edu.cn (X. Shen).

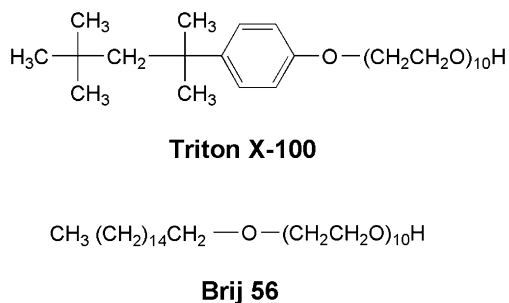


Fig. 1. Chemical structures of Triton X-100 and Brij 56.

tween the reduction rate of Cu^{2+} depending on the yield of e_{aq}^- and the escape rate of the mixed solvent.

2. Materials and methods

2.1. Chemicals

Triton X-100 (CP, Beijing Chemical Reagents Inc.) and Brij 56 (Aldrich), as shown in Fig. 1, were used as received. Cyclohexane (AR, Beijing Chemical Reagents Inc.), toluene, ethylene glycol (EG, AR, Beijing Chemical Plant), *n*-hexanol, and copper nitrate (AR, Beijing Yili Fine Chemical Products Inc.) were used without further purification. Deionized and tridistilled water was used in the experiments.

2.2. Synthesis of nanocubes

A certain amount of $\text{Cu}(\text{NO}_3)_2$ was dissolved in the mixed solvent of EG and water (molar ratio 1:7.23) to make up a 0.02 mol L^{-1} stock solution. To prepare microemulsions, surfactant (Triton X-100 or Brij 56), *n*-hexanol, and cyclohexane (molar ratio 1.0:1.6:57.6) were first mixed and then a certain volume of stock solution was added, with the molar ratio of water to surfactant (ω) fixed at 6.3. The mixtures were stirred at room temperature until they became transparent. After bubbling with high-purity N_2 under anaerobic conditions, the microemulsions were irradiated in the field of a ^{60}Co γ -ray source for 16 h and 40 min, with an absorbed dosage of 40 kGy. Then, after centrifugation, orange-red precipitates and yellowish solutions were obtained.

2.3. Characterization

After irradiation, the absorption spectra were immediately recorded on a U-3010 spectrometer, with identical systems that had not been irradiated as standard. Thereafter, the samples were de-emulsified and washed with ethanol and then dispersed in ethanol. The obtained dispersion was dropped onto a carbon-coated copper grid. After the solvent was evaporated at room temperature, the transmission electron microscopy (TEM) and selected area electron diffraction (SAED) images were obtained on a JEOL JEM-200CX microscope operated at 160 kV, high-resolution TEM (HRTEM) images were obtained on a Hitachi 9000 transmission electron microscope operated at 300 kV, and scanning electron microscopy (SEM) images were obtained via

an AMARY 1910FE scanning electron microscope operated at 15 kV. The range of nanoparticle sizes was determined after measuring the dimensions of more than 500 nanoparticles based on the obtained micrographs. After the dispersed sample was deposited on a piece of glass, powder X-ray diffraction (XRD) pattern was recorded on an X'Pert PRO MPD diffractometer with $\text{CuK}\alpha$ radiation ($\lambda = 0.15418 \text{ nm}$) and an X-ray photoelectron spectrum (XPS) was collected on a Kratos Axis Ultra spectrometer with monochromatized $\text{AlK}\alpha$ radiation.

3. Results

3.1. Formation of solid nanocubes in the Triton X-100-based microemulsion

Fig. 2A (curve a) shows the UV–vis spectrum of the reduction product of $\text{Cu}(\text{NO}_3)_2$ in the Triton X-100-based microemulsion. The broad absorption with a peak at ca. 510 nm can be ascribed to the characteristic absorption of Cu_2O [12,28], suggesting the generation of Cu_2O in the irradiation course. The corresponding XRD pattern is shown in Fig. 2B (curve a). The interplanar distances calculated for (110), (111), (200), (220), and (311) from the XRD pattern match well with the standard data of cubic phase Cu_2O (JCPDS File 05-0667), confirming the formation of cubic phase Cu_2O . The fact that the (200) peak is significantly intensified suggests a preferential alignment of the (100) plane parallel to the specimen surface. The corresponding XPS analysis (curve a in Fig. 2C) shows that the kinetic energy of Cu LMM is 916.3 eV, close to the value of Cu_2O in the literature [29], which further confirms the generation of Cu_2O . Besides, the Cu LMM peak characterizing Cu(0), which is usually centered at about 918.6 eV [29], is not found in Fig. 2C (curve a), indicating the absence of metallic Cu in the reduction product. It can be seen from TEM (Fig. 3A) and SEM images (Fig. 4A) that the as-prepared products are mainly composed of nanocubes, with the edge length ranging from 80 to 120 nm. These nanocubes further construct a local ordered structure spontaneously (Fig. 3A), which can be further observed via the corresponding SEM image (Fig. 4A). The typical HRTEM image shown in Fig. 5A exhibits clear lattice fringes with d spacing of 0.30 nm, which corresponds to (110) reflection of the cubic Cu_2O structure, confirming the formation of crystalline Cu_2O nanoparticles. The inset of Fig. 3A is a typical SAED pattern of a related solid nanocube, which indicates a highly preferred {001} orientation texture structure. It is also noticed that additional tional s-319difofts[(from)-3dc

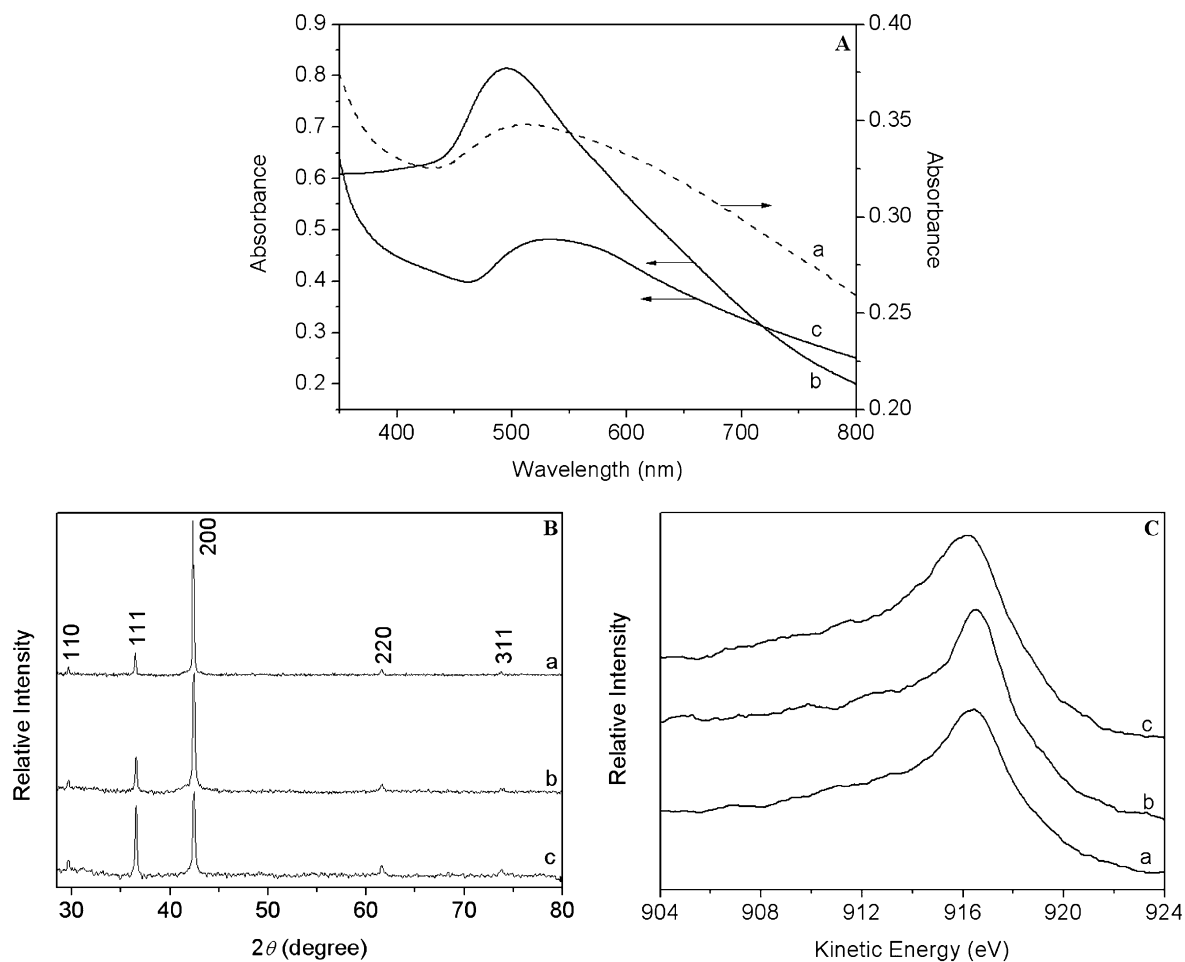


Fig. 2. UV-vis spectra (A), XRD patterns (B), and Cu LMM Auger spectra (C) of the reduction products of $\text{Cu}(\text{NO}_3)_2$ in the Triton X-100-based microemulsion (a), and in the Brij 56-based microemulsions in the absence (b), and presence (c) of toluene ($[\text{toluene}] = 1.86 \text{ mol L}^{-1}$).

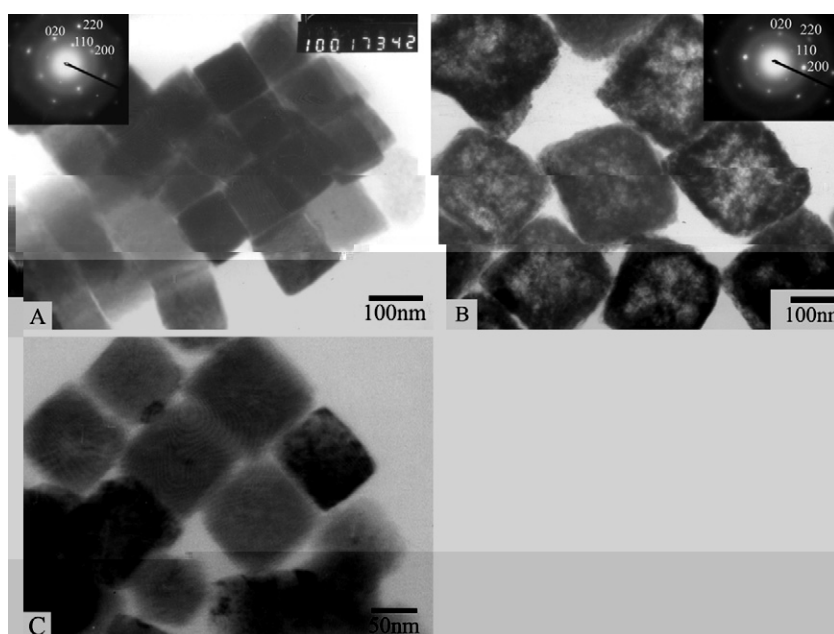


Fig. 3. TEM images of the reduction products of $\text{Cu}(\text{NO}_3)_2$ in the Triton X-100-based (A, C) or Brij 56-based (B) microemulsions. The inset shows the SAED pattern of the corresponding product.

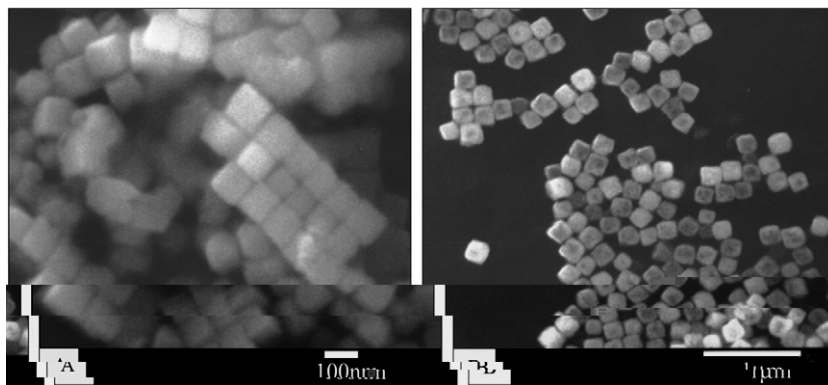


Fig. 4. SEM images of the reduction products of Cu(NO₃)₂ in the Triton X-100-based (A) or Brij 56-based (B) microemulsions.

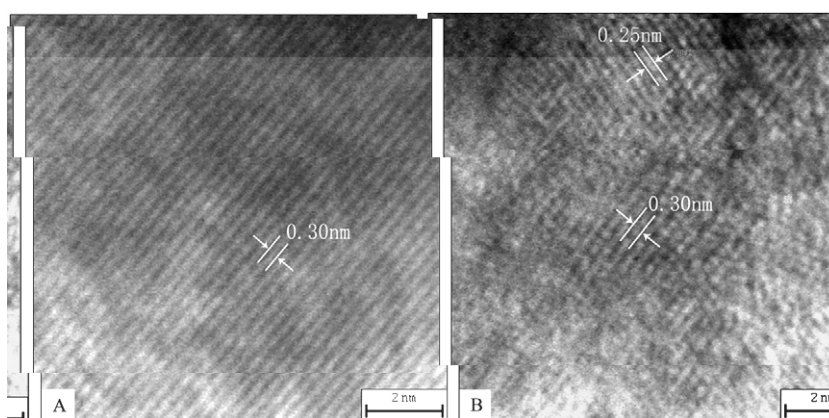


Fig. 5. HRTEM images of the reduction product of Cu(NO₃)₂ in the Triton X-100-based microemulsion.

3.2. Formation of hollow nanocubes in the Brij 56-based microemulsion

When Triton X-100 was replaced with Brij 56 in the microemulsion, a similar UV–vis spectrum (curve b in Fig. 2A), XRD pattern (curve b in Fig. 2B), Cu LMM Auger spectrum (curve b in Fig. 2C), SAED pattern (inset, Fig. 3B), and HRTEM images (not shown) were obtained, indicating the generation of Cu₂O nanoparticles. The corresponding TEM (Fig. 3B) and SEM (Fig. 4B) images show that the edge length of the nanocubes ranges from 130 to 210 nm. In addition, the TEM image (Fig. 3B) shows a distinct contrast between the dark edge and the pale center in most nanocubes, evidencing their hollow nature. The wall thickness is estimated to be 20–50 nm. In the absorption spectrum, the broad absorption peak is blue-shifted to about 495 nm. As is well known, the absorption band of nanoparticles is affected by the quantum size effect (QSE) [1,28]. If the QSE is related to the size of the edge length as solid nanoparticles, the hollow particles are too large to observe an obvious QSE. It may be the thickness of the hollow Cu₂O nanocubes' wall that is related to QSE, which causes the blue shift of the Cu₂O absorption peak.

3.3. Effect of toluene

It is strange that the morphologies of the reduction products of Cu(NO₃)₂ in the two microemulsions are markedly different, although the structures of the two nonionic surfactants are similar. After examination of their molecular structures, it can easily be found that a phenyl ring exists in the hydrophobic chain of Triton X-100. It was reported that toluene can react with the excess electrons in cyclohexane, with a rate constant of 4.0×10^9 L mol⁻¹ s⁻¹.

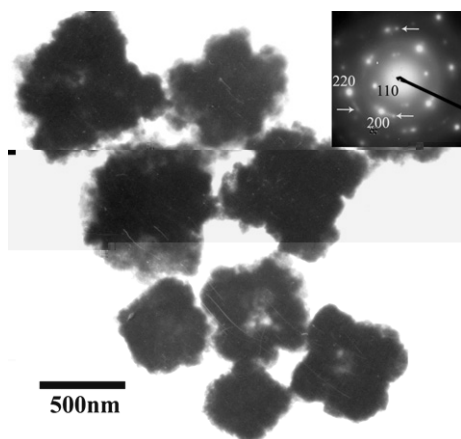


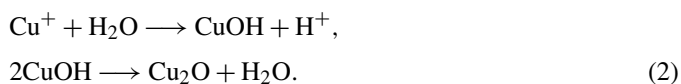
Fig. 6. TEM image of the reduction product of $\text{Cu}(\text{NO}_3)_2$ in the Brij 56-based microemulsion in the presence of toluene (1.86 mol L^{-1}). The inset shows the SAED pattern.

4. Discussion

In the radiolytic reduction of Cu^{2+} , e_{aq}^- plays the main role. First, e_{aq}^- reduces Cu^{2+} to Cu^+ :



Then, Cu_2O is generated through the hydrolysis of Cu^+ :



At the same time, the disproportionation,



and the further reduction,



of Cu^+ are two important competing reactions, which can be suppressed by reducing the yield of e_{aq}^- [27]. During the irradiation of microemulsions, e_{aq}^- can be generated mainly from the scavenging of excess electrons, which are produced originally through the radiolysis of oil, by the water pool [27,31–34]. In addition, the radiolysis of water in the water pool can generate e_{aq}^- directly, but it is less important [27,31–34].

According to the results in the literature [31–38] and in our previous work [27], the ω value, the kind of anion, the viscosity

very small number, e.g., 1–3, of copper ions exist in each water pool, depending on the average aggregation number of the surfactant. Thus, the growth of Cu_2O nanoparticles must experience a mass exchange course between water pools. The presence of EG can reduce the rigidity of the interface of a W/O microemulsion [39], similarly to the action of short-chain alcohol [40] and benzyl alcohol [40,41]. This will favor the above-mentioned mass exchange. In the Brij 56-based microemulsion with EG, although the reactivity of e_{aq}^-

- [26] J.X. Huang, Y. Xie, B. Li, Y. Liu, Y.T. Qian, S.Y. Zhang, *Adv. Mater.* 12 (2000) 808.
- [27] Q.D. Chen, X.H. Shen, H.C. Gao, *J. Colloid Interface Sci.* 308 (2007) 491.
- [28] P. He, X.H. Shen, H.C. Gao, *J. Colloid Interface Sci.* 284 (2005) 510.
- [29] J.F. Moulder, W.F. Stickle, P.E. Sobol, K.D. Bomben, *Handbook of X-ray Photoelectron Spectroscopy*, Perkin–Elmer Physical Electronics Division, Eden, 1992, p. 203.
- [30] V.I. Tupikov, in: V.K. Milinchuk, V.I. Tupikov (Eds.), *Organic Radiation Chemistry Handbook*, Ellis Horwood Ltd. Chichester, 1989, p. 46.
- [31] M. Wong, M. Gratzel, J.K. Thomas, *Chem. Phys. Lett.* 30 (1975) 329.
- [32] J.L. Gebicki, L. Gebicka, J. Kroh, *J. Chem. Soc. Faraday Trans.* 90 (1994) 3411.
- [33] S. Adhikari, R. Joshi, C. Gopinathan, *J. Colloid Interface Sci.* 191 (1997) 268.
- [34] R. Joshi, T. Mukherjee, *Radiat. Phys. Chem.* 66 (2003) 397.
- [35] M.P. Pileni, B. Hickel, C. Ferradini, J. Pucheault, *Chem. Phys. Lett.* 92 (1982) 308.
- [36] M.P. Pileni, P. Brochette, B. Hickel, B. Lerebours, *J. Colloid Interface Sci.* 98 (1984) 549.
- [37] G.V. Buxton, C.L. Greenstock, W.P. Helman, A.B. Ross, *J. Phys. Chem. Ref. Data* 17 (1988) 513.
- [38] V. Calvo-Perez, G.S. Beddard, J.H. Fendler, *J. Phys. Chem.* 85 (1981) 2316.
- [39] L. Garcia-Rio, J.R. Leis, J.C. Mejuto, M.E. Pena, E. Iglesias, *Langmuir* 10 (1994) 1676.
- [40] S. Modes, P. Lianos, *J. Phys. Chem.* 93 (1989) 5854.
- [41] R.P. Bagwe, K.C. Khilar, *Langmuir* 13 (1997) 6432.
- [42] O. Celik, O. Dag, *Angew. Chem. Int. Ed.* 40 (2001) 3799.
- [43] Z.B. Huang, F.Q. Tang, *J. Colloid Interface Sci.* 275 (2004) 142.